

# QRS DETECTION IN COMPUTER-BASED ECG SIGNAL ANALYSIS USING THE HILBERT TRANSFORM

**D Benitez MSc.‡, P Gaydecki PhD.‡, A Zaidi MRCP.§, AP Fitzpatrick MD. FACC.§**

‡ Department of Instrumentation and Analytical Science, University of Manchester Institute of Science and Technology (UMIST), Manchester, U.K.

§ Manchester Heart Centre, The Royal Infirmary, Manchester, U.K.

**Keywords:** QRS Detection, Hilbert Transform, Noise Stress Test.

## Abstract

A new robust algorithm for locating the R wave peaks in computer-based ECG analysis using the properties of the Hilbert transform is presented in this paper. The method developed for QRS complex detection allows the differentiation of R waves from large, peaked T and P waves with a high degree of accuracy and minimizes the problems associated with baseline drifts, motion artifacts and muscular noise. The performance of the algorithm was tested using standard noise free and noise contaminated ECG waveform records from the MIT-BIH Arrhythmia Database. A detection error rate of less than 0.5 % was achieved in every studied case. The reliability of the proposed detector is also compared with published results for other QRS detectors. The noise tolerance of the new proposed QRS detector was also tested using standard records from the MIT-BIH Noise Stress Test Database. The sensitivity of the detector remains about 90% even for SNR's as low as 6dB.

## 1. Introduction

Accurate determination of the QRS complex, in particular, accurate detection of the R wave peak, is essential in computer-based ECG analysis. However, this is often difficult to achieve, since noise contamination due to baseline drifts, motion artifacts and muscular noise, is frequently encountered [1].

Contact author: Diego Benitez  
DIAS, UMIST,  
PO Box 88, Manchester M60 1QD, UK.  
Phone: (44) 161 200 8902  
Fax: (44) 161 200 4911  
e-mail: [diego.benitez@stud.umist.ac.uk](mailto:diego.benitez@stud.umist.ac.uk)

Morphological differences in the ECG waveform also increase the complexity of the QRS detection process, due to the high degree of heterogeneity in the QRS waveform and the difficulty in differentiating the QRS complex from tall peaked P or T waves [2]. Different approaches have been used to improve the accuracy of QRS detection, including the use of the Hilbert transform.

The use of the Hilbert transform in ECG analysis was first introduced by Bolton and Westphal [3]-[6]. In general, the method they proposed uses two-dimensional graphical representations like vectorcardiographs and polarcardiographs to examine the concept of pre-envelope and envelope of a real waveform given by the Hilbert transform. They developed a prototype two stage QRS detector based on the determination of a zero crossing in the Hilbert transformed data of the original ECG waveform coincident with a large magnitude in its envelope.

A new approach to QRS detection using other properties of the Hilbert transform is presented in this paper. The algorithm uses the first differential of the ECG signal and its Hilbert transformed data to find regions of high probability and to locate the R peaks in the ECG waveform. Similar to the Bolton and Westphal's method, a second stage detection algorithm uses these initial estimations to locate the real R peaks in the ECG wave. This has a number of advantages over previously described techniques. The unwanted effects of large peaked T and P waves are minimized and the new algorithm performs excellently in the presence of significant noise contamination. Moreover, in contrast to Bolton and Westphal's method, determination of the envelope and pre-envelope of the given data is not required.

## 2. The Hilbert Transform

Given a real time function  $x(t)$ , its Hilbert transform [7]-[8] is defined as:

$$\hat{x}(t) = H[x(t)] = \frac{1}{\pi} \int_{-\infty}^{\infty} x(\tau) \frac{1}{t-\tau} d\tau \quad (1)$$

It can be seen from (1) that the independent variable is not changed as result of this transformation, so the output  $\hat{x}(t)$  is also a time dependent function. Furthermore,  $\hat{x}(t)$  is a linear function of  $x(t)$ . It is obtained from  $x(t)$  applying convolution with  $(\pi t)^{-1}$  as shown in the following relationship:

$$\hat{x}(t) = \frac{1}{\pi t} * x(t) \quad (2)$$

Rewriting Equation (2) and applying the Fourier transform, we have:

$$F\{\hat{x}(t)\} = \frac{1}{\pi} F\left\{\frac{1}{t}\right\} F\{x(t)\} \quad (3)$$

Since,

$$F\left\{\frac{1}{t}\right\} = \int_{-\infty}^{\infty} \frac{1}{x} e^{-t^2 \pi x dx} = -j\pi \operatorname{sgn} f \quad (4)$$

$$\text{where: } \operatorname{sgn} f = \begin{cases} +1 & f > 0 \\ 0 & f = 0 \\ -1 & f < 0 \end{cases}$$

The Fourier transform of the Hilbert transform of  $x(t)$  given by Equation (3) may be re-expressed as:

$$F\{\hat{x}\} = -i \operatorname{sgn} f F\{x(t)\} \quad (5)$$

In the frequency domain, the result is then obtained by multiplying the spectrum of the  $x(t)$  by  $j$  ( $+90^\circ$ ) for negative frequencies and  $-j$  ( $-90^\circ$ ) for positive frequencies. The time domain result can be obtained performing an inverse Fourier transform. Therefore, the Hilbert transform of the original function  $x(t)$  represents its harmonic conjugate [8]. The concept of analytic signal or pre-envelope of a real signal  $x(t)$  [9], is described by the expression:

$$y(t) = x(t) + j\hat{x}(t) \quad (6)$$

The envelope  $B(t)$  of  $y(t)$  is defined by:

$$B(t) = \sqrt{x^2(t) + \hat{x}^2(t)} \quad (7)$$

and its instantaneous phase angle in the complex plane can be defined by:

$$\phi(t) = \arctan\left(\frac{\hat{x}(t)}{x(t)}\right) \quad (8)$$

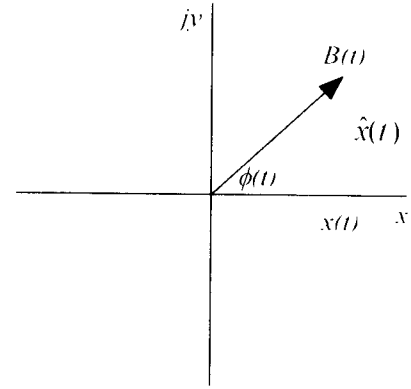


**Figure 1 Complex representation of the envelope.**

As shown in Figure 1,  $B(t)$  and  $x(t)$  have common tangents and the same values at the points where  $\hat{x}(t) = 0$ , i.e. the envelope determined using Equation (7) will have the same slope and magnitude of the original signal  $x(t)$  at or near its local maxima. Similarly, from Equation (7) it can be seen that  $B(t)$  is always a positive function. Hence, the maximum contribution to  $B(t)$  at points where  $x(t) = 0$  is given by the Hilbert transform. This can be easily seen in Figure 2 where the maximum contribution to the envelope of the first differential of the ECG  $B(d/dt ECG)$  is given by its Hilbert transform  $H[d/dt ECG]$  at points where  $d/dt ECG = 0$ .

## 3. The new Approach to QRS detection using the Hilbert transform

One of the properties of the Hilbert transform is that it is an odd function. That is to say that it will cross zero on the x-axis every time that there is an inflexion point in the original waveform (Figure 2). Similarly a crossing of the zero between consecutive positive and negative inflexion points in the original waveform will be represented as a peak in its Hilbert transformed conjugate.

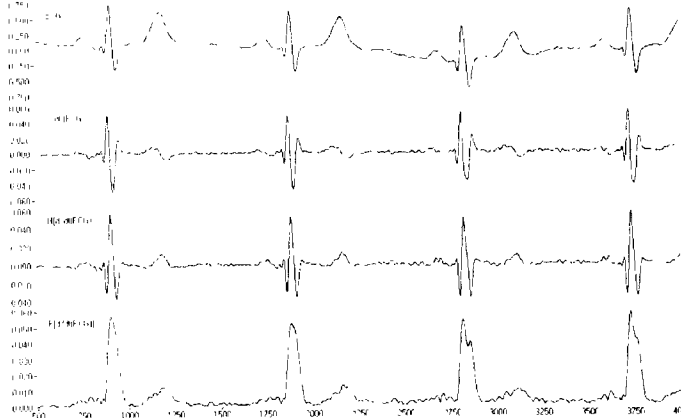


**FIGURE 2 ECG Contributions to the envelope  $B[d/dt(ECG)]$ , where  $d/dt(ECG)$  is the first differential of the ECG waveform and  $H(d/dt(ECG))$  is its Hilbert transform.**

This interesting property can be used to develop an elegant and much easier way to find the peak of the QRS complex in the ECG waveform corresponding to a zero crossing in its first differential waveform  $d/dt(ECG)$ . The block diagram of the proposed approach is shown in Figure 3.

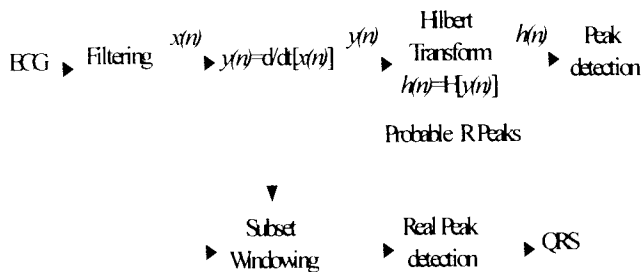


**Figure 3 Block diagram of the QRS detector.**

As with most QRS detector algorithms, the first stage of the proposed algorithm is formed by a filtering section [10]. We used a band pass FIR filter windowed using a Kaiser-Bessel window. The band stop frequencies were set at 8 and 20 Hz in order to remove muscular noise and maximize the QRS complex respectively. Then, the first differential of the resulting filtered sequence was performed in order to remove motion artifacts and base line drifts. The rising slope of the R wave is represented as a maximum and the falling slope will be represented as a minimum in the first differential sequence. The peak of the R wave will be equivalent to the zero crossing between these two positive and negative peaks (see Figure 2).

So given the filtered ECG waveform sequence  $x(n)$ , its first differential ( $y(t)=d/dt(ECG)$ ) in discrete domain can be obtained by:

$$y(n) = \frac{1}{2\Delta t} [x(n+1) - x(n-1)] \quad (9)$$

for  $n = 0, 1, 2, \dots, m-1$

where:  $m$  is the total number of samples  
 $\Delta t$  is the sampling frequency

The initial condition is specified by  $x(-1)$  when  $n = 0$ , and the final condition  $x(m)$  when  $n = m-1$ .

These conditions minimize the error at the boundaries.

The Hilbert transform  $h(n)$  of the sequence  $y(n)$  that represents the first differential of the ECG waveform is then obtained using the following methodology:

1. Obtain the Fourier transform  $F(n)$  of the input sequence  $y(n)$
2. Set the DC component to zero
3. Multiply the positive and negative harmonics by  $-j$  and  $j$  respectively
4. Perform the inverse Fourier transform of this resulting sequence.

Since this algorithm for Hilbert transformation works well with short sequences, a moving 1024 points window is used to subdivide the input sequence  $y(n)$  before obtaining its Hilbert transform. To optimise accuracy, the starting point of the next window should match the last R point located in the previous ECG subset.

The peaks in the Hilbert transformed sequence  $h(n)$  represent regions of high probability of finding a real QRS peak. In practice, these peaks often differ from the true R wave peak position by a few milliseconds. In order to guarantee accurate detection of the R peaks, a second stage detector is required. Because the P and T waves are minimized in relation to the relative peak corresponding to QRS complex in the Hilbert sequence, a simple threshold detection is used to locate the peaks in the  $h(n)$  sequence.

The second stage detector uses the information provided by the first approximation. A pre-defined window width subset (i.e.  $\pm 10$  samples from the location of the peak found in the corresponding  $h(n)$  sequence) is selected in the original ECG waveform to locate the real R peak. Once again a simple

maximum peak locator in the values of this subset sequence is used.

#### 4. Methods

The detector was tested using entire records from the MIT-BIH Arrhythmia database [11]. From this database, a set of noiseless and noisy ECG waveforms was chosen to test the performance of the new algorithm. These signals were recorded using the modified limb lead II (MLII) ECG electrode configuration, and contain mechanical and electrical artifacts. Beat by beat comparison was performed according to the recommendation of the American National Standard for ambulatory ECG analysers (ANSI/AAMI EC38-1994) [12]. A false negative (FN) occurs when the algorithm fails to detect a true beat (actual QRS) quoted in the corresponding annotation file of the MIT-BIH record and a false positive (FP) represents a false beat detection. Sensitivity (Se) [12], positive prediction (+P) [12], and detection error rate (*DER*) [13] were calculated using equation 12 to 14 respectively:

$$\text{Sensitivity (\%)} = \frac{TP}{TP + FN} \% \quad (12)$$

$$\text{Positive predictivity (\%)} = \frac{TP}{TP + FP} \% \quad (13)$$

$$\text{DER (\%)} = \frac{FP + FN}{\text{Total \# of QRS complex}} \% \quad (14)$$

Where: TP (true positives) is the total number of QRS correctly located by the detector.

The chosen records for the analysis and their respective characteristics are described in Table 1.

MIT-BIH Record	Characteristics
100	Normal sinus rhythm
105	High noise and artifacts
111	Noise + baseline wander
113	Baseline wander
114	Baseline artifacts
118	Moderate noise
119	Moderate noise

**Table 1 MIT-BIH Records Selected for the Analysis.**

The noise effects in the detector were quantified by the noise stress test recommended by the ANSI/AAMI EC38-1994 standard using the records from the MIT-BIH Noise Stress Test Database [11]. This database contains 12 sample records contaminated with electrode motion artifact, usually as the result of intermittent mechanical forces acting on the electrodes, and significant amount of baseline wander and muscular noise. The signal-to-noise ratios (SNR) of the noisy files of this database are summarized in Table 2.

Record	SNR (dB)	Record	SNR (dB)
118e24	24	119e24	24
118e18	18	119e18	18
118e12	12	119e12	12
118e06	6	119e06	6
118e00	0	119e00	0
118e_6	-6	119e_6	-6

**Table 2 Records of the MIT-BIH Noise Stress Test Database.**

#### 5. Results and discussion

The detector shows outstanding performance for noisy signals even in the presence of pronounced muscular noise and baseline artifacts. The results obtained for the testing records are shown in Table 3. In the case of the noise tolerance test, the performance of the proposed QRS detector remains high for SNR's as low as 6 dB with high sensitivity values (about 90%) and with equally high positive predictions (above 88%). The results obtained are presented in Table 4.

The sensitivity of the detector falls under 90% for SNR's lower than 6dB. The reliability of the proposed detector compares very favourably with published results for other QRS detectors especially for the difficult to analyse noisy MIT-BIH record 105. The predominant features of this record are high grade of noise and artifacts [11]. Comparative results are shown in the Table 5.

#### 5. Conclusion

The usefulness of the properties of the Hilbert transform for QRS detection has been studied in this paper and a new QRS complex detector has been proposed. Using the MIT-BIH arrhythmia database, the algorithm developed performed highly effectively with accurate QRS peak detection, even in the

presence of significant noise contamination. This robust noise rejection of the algorithm proposed is emphasized with the results obtained for the noise stress test, where high sensitivity and positive prediction rates were obtained for even high noise contaminated signals.

MIT-BIH record	Actual number of beats in record	FP	FN	Failed detection (FP+FN)	Detection error rate %	Se (%)	+P (%)
100	2273	0	0	0	0.00	100	100
105	2572	7	3	10	0.39	99.88	99.73
111	2124	1	1	2	0.09	99.95	99.95
113	1795	0	0	0	0.00	100	100
114	1879	1	0	1	0.05	100	99.95
118	2278	0	0	0	0.00	100	100
119	1987	0	0	0	0.00	100	100

**TABLE 3. QRS Detection Performance using the MIT-BIH Database.**

MIT-BIH Noise Stress Test record	Actual number of beats in record	FP	FN	Failed detection (FP+FN)	Detection error rate %	Se (%)	+P (%)
118e24	2278	0	0	0	0.00	100	100
118e18	2278	4	1	5	0.22	99.96	99.82
118e12	2278	63	27	90	3.95	98.81	97.28
118e06	2278	210	121	331	14.53	94.69	91.13
118e00	2278	402	361	763	33.49	84.15	82.66
118e_6	2278	529	491	1020	44.78	78.45	77.16
119e24	1987	1	0	1	0.05	100	99.95
119e18	1987	4	1	5	0.25	99.95	99.80
119e12	1987	101	17	118	5.94	99.14	95.12
119e06	1987	239	82	321	16.16	95.87	88.85
119e00	1987	409	204	613	30.85	89.73	81.34
119e_6	1987	561	376	937	47.16	81.08	74.17

**TABLE 4. Noise Tolerance of the proposed QRS Detector Using the MIT-BIH Noise Stress Test Database.**

Method	FP	FN	Failed detection	Detection error rate %	Se %	+P %	Reference
Proposed detector	7	3	10	0.39	99.88	99.73	
Neural-based adaptive filtering	10	4	14	0.54	99.84	99.61	[13]
Wavelet transforms	15	13	28	1.09	99.50	99.42	[14]
Topological mapping	41	4	45	1.75	99.84	98.43	[15]
Optimised filtering and dual edge thresholding	35	21	56	2.18	99.19	98.66	[16]
Linear adaptive filtering	40	22	62	2.41	99.15	98.47	[13]
Bandpass filtering and search-back	53	22	75	2.91	99.15	97.98	[10]
Bandpass filtering	67	22	89	3.46	99.15	97.46	[17]
Filter banks*	53	16	69	3.22	99.26	97.58	[18]

\* This result reporter over 2139 beats only.

**TABLE 5. Performance Comparison with other Detectors for the noisy MIT-BIH record 105 containing 2572 QRS complex.**

## REFERENCES

- [1] Friesen, G.M., Jannett, T.C., Jadallah, M.A., Yates, S.L., Quint, S.R., Nagle, H.T., *A comparison of the noise sensitivity of nine QRS detection algorithms*. IEEE Trans. Biomed. Eng., vol. 37, pp.85-98, 1990.
- [2] Thakor, N.V., Webster, J.G., Thompkins, W.J., *Estimation of QRS complex power spectra for design of a QRS filter*, IEEE Trans. Biomed. Eng., vol. BME-31, pp.702-705, 1984.
- [3] Bolton, R.J., Westphal, L.C., *Hilbert transform processing of ECG's*, 1981 IREECON International Convention Digest, pp.281-283, Melbourne: IREE, 1981.
- [4] Bolton, R.J., Westphal, L.C., *Preliminary results in display and abnormality recognition of Hilbert Transformed e.c.g.s*, Medical and Biomedical Engineering and Computing, No.3, pp.377-388, 1981.
- [5] Bolton, R.J., Westphal, L.C., *On the use of the Hilbert Transform for ECG waveform processing*, Computers in Cardiology, pp.533-536, Long Beach: IEEE Computer Society, 1984.
- [6] Bolton, R.J., Westphal, L.C., *ECG display and QRS detection using the Hilbert Transform*, Computers in Cardiology, No.1985, pp.463-466, 1985.
- [7] Bracewell, R.N., *The Fourier transform and its applications*, McGraw-Hill, pp.267-274, 1978.
- [8] Analogic, *Universal waveform analyser. Application note #301 (Advanced Math)*, Analogic Ltd., pp.1301-1-1301-5.
- [9] Oppenheim, A.V., Schaffer, R.W., *Discrete-Time Signal Processing*, Englewood Cliffs, NJ, Prentice-Hall, 1989.
- [10] Hamilton, P.S., Tompkins, W.J., *Quantitative investigation of QRS detection rules using the MIT/BIH arrhythmia database*, IEEE Trans. Biomed. Eng., vol. BME-33, pp.1157-1165, 1986.
- [11] *MIT-BIH Database distribution*, Massachusetts Institute of Technology, 77 Massachusetts Avenue, Cambridge, MA 02139, 1998.
- [12] *American National Standard for Ambulatory Electrocardiographs*, publication ANSI/AAMI EC38-1994, Association for the Advancement of Medical Instrumentation, 1994
- [13] Xue, Q., Hu, Y.H., Tompkins, W.J., *Neural-network-based adaptive matched filtering for QRS detection*, IEEE Trans.

Biomed. Eng., vol. BME-39, pp. 315-329, 1992.

- [14] Li, C., Zheng, C., Tai, C., *Detection of ECG characteristic points using wavelet transforms*, IEEE Trans. Biomed. Eng., vol. 42, No.1, pp. 21-28, 1995.
- [15] Lee, J., Jeong, K., Yoon, J., Lee, M., *A simple real-time QRS detection algorithm*, Proceedings of the 18th Annual International Conference of the IEEE Engineering in Medicine and Biology Society, Amsterdam 1996.
- [16] Ruha, A., Sallinen, S., Nissila, S., *A real-time microprocessor QRS detector system with a 1-ms timing accuracy for the measurement of ambulatory HRV*, IEEE Trans. Biomed. Eng., vol. 44, pp.159-167, 1997.
- [17] Pan, J., Tompkins, W.J., *A real time QRS detection algorithm*, IEEE Trans. Biomed. Eng., vol. BME-32, no.3, pp.230-236, 1985.
- [18] Afonso, V.X., Tompkins, W.J., Nguyen, T.Q., Luo, S., *ECG beat detection using filter banks*, IEEE Trans. Biomed. Eng., vol. 46, no.2, pp.192-201, 1999.

## Biographies



**Diego S. Benitez** was born in Quito, Ecuador on January 9, 1970. He received his Engineering degree in Electronics and Control from the Escuela Politecnica Nacional, Quito, Ecuador in 1994, and a MSc. degree in

Instrumentation and Analytical Sciences (Digital Instrumentation and Signal and Image Processing) from The University of Manchester Institute of Science and Technology (UMIST), Manchester, UK, in 1997. He is presently completing his PhD studies in Instrumentation and Digital Signal Processing (DSP) at UMIST. His professional interests are in DSP, intelligent sensor systems, biomedical instrumentation, microcontrollers, control systems, industrial automation, digital systems and computing. Mr. Benitez is member of the IEEE and of the Institute of Physics.

**Dr. Patrick Gaydecki** is a Senior Lecturer in the Department of Instrumentation and analytical Science at UMIST. He gained a 1st Class Honours Degree in Computing and Biology from the University of Demontfort in 1980, and his PhD in Ecological Physics from the University of Cranfield in 1984. He is chartered physicist, a member of the Institute of Physics and the British Institute of Nondestructive Testing and is also currently Honorary Editor of the journal *Nondestructive Testing and Evaluation*. He leads a research team of ten individuals, which conducts research and development into signal and image processing solutions for nondestructive testing, medical, and audio-bandwidth signal applications. These solutions take the form of sensor design, electronic system design, in particular digital systems design, and the production of signal and image processing software. He has a keen interest in the development of real-time Digital Signal Processing (DSP) hardware and software, based around modern high MIP-rate DSP devices. He has published over 60 papers relating to signal processing, having presented his work in Europe and the Americas. He regularly presents public lectures at UMIST, and was recently been invited to give a keynote address to the *Physics Congress 2000*, an international event organized by the Institute of Physics in the UK.

